esa

ECOSPHERE

Thermal biology and growth of bison (*Bison bison*) along the Great Plains: examining four theories of endotherm body size

JEFF M. MARTIN [1,†] AND PERRY S. BARBOZA [1,2]

[1]*Department of Ecology and Conservation Biology, Texas A&M University, College Station, Texas 77843-2258 USA*
[2]*Department of Rangeland, Wildlife, and Fisheries Management, Texas A&M University, College Station, Texas 77843-2258 USA*

Citation: Martin, J. M., and P. S. Barboza. 2020. Thermal biology and growth of bison (*Bison bison*) along the Great Plains: examining four theories of endotherm body size. Ecosphere 11(7):e03176. 10.1002/ecs2.3176

Abstract. Body size of bison (*Bison bison*) declines with rising global temperature across the fossil record and rising annual temperatures across the Great Plains, but what are the underlying drivers? Body size depends on growth, which depends on maximizing net energy and nutrient flows for the production of tissues at seasonal scales across the range of the species. We measured thermoregulation costs of body surface temperature (°C) and heat exchanges (W and W/m^2) of 350 adult and 345 adolescent *Bison* from 19 herds in summer and winter along the Great Plains from Saskatchewan (52° N) to Texas (30° N). At the smallest scale, daily body surface temperature increased with solar radiation and decreased with relative humidity and wind speed, which is consistent with Kooijman's dynamic energy budget theory. Total surface heat transfer (W) increased with body mass (kg) at an exponent of 0.63 ± 0.03, which is consistent with Schmidt-Nielsen's principle of surface-area-to-volume ratios (b = 0.67). On an annual scale, growth (kg/yr) of adolescent *Bison* decreased with increasing total surface heat transfer (W) during summer, which supports Speakman and Król's heat dissipation limit theory. On the largest scale, heat flux was weakly related to latitude in summer and winter for adolescent *Bison*, which provides support for Bergmann's rule and suggests a role for local primary production along the Great Plains. Cooler summers are more optimal for *Bison* growth because of reduced heat loads during the growing season. Rising temperatures are likely to constrain body size and productivity of *Bison* and other large endotherms in North America.

Key words: allometry; Bergmann's rule; body size; climate change; dynamic energy budget; Great Plains; growth; heat dissipation limit; thermogrammetry.

Received 4 March 2020; revised 8 April 2020; accepted 13 April 2020; final version received 19 May 2020. Corresponding Editor: Robert R. Parmenter.

† **E-mail:** jeff.m.martin@tamu.edu

INTRODUCTION

Body size of bison (*Bison bison*) has shrunk by 31% (Martin et al. 2018) with rising mean global temperature since the last Ice Age, and over the last 5 decades, body size of *Bison* has declined by 11–23% (Martin and Barboza 2020) with rising mean annual temperature along the Great Plains of North America, but what are the mechanisms driving temperature response? Maximum body size of endotherms depends on optimal growth of individuals and thus populations. Optimal growth depends on low costs of maintenance for the efficient production of tissues, especially in seasonal environments when food availability and environmental demands constrain the annual window for growth. High thermal loads increase costs of body maintenance to balance internal and external heat loads through thermoregulation, which ultimately reduces the energy available for growth. Heat loads are measured by heat flux (W/m^2) which measures the exchange of thermal energy between an animal

and their environment. Here, we describe heat flux (W/m^2) and total surface heat transfer (W) of *Bison* as measures of thermal energy balance at small timescales and growth at seasonal and annual scales of time. Thermal balance is central to four theories that attempt to explain the change in body size of animals with warming from small to large scales of organization, space, and time:

1. Kooijman's dynamic energy budget hypothesis (Kooijman 2000, Kearney 2012)
2. Schmidt-Nielsen's body surface-area-to-volume ratio (Schmidt-Nielsen 1970)
3. Speakman and Król's heat dissipation limit hypothesis (Speakman and Król 2010, 2011)
4. Bergmann's rule (Bergmann 1847, Clauss et al. 2013)

Kooijman's dynamic energy budget theorized that energy balances and thus micro-climates and weather affected heat transfer and energy use of animals on the landscape to ultimately affect life history. Schmidt-Nielsen theorized that allometric scaling of surface-area-to-volume ratio ($b = 0.67$) increased heat retention as animals increased body size, which would favor survival in cold environments for larger animals. Speakman and Król theorized that heat dissipation limits to thermoregulatory costs under rising heat loads limited reproduction and growth and affects life history and body size of animals. Bergmann's rule predicts thermal conservatism of animals for cooler climates at higher latitudes will produce larger individuals within and across species than warmer climates at lower latitudes.

The theories of Bergmann and Schmidt-Nielsen emphasize selection for survival by reducing heat flux that results in a net loss of energy from the body during extreme cold and prolonged winters. The theories of Kooijman, Speakman and Król emphasize selection for growth and reproduction by controlling excessive heat flux during a short summer window of food availability with heat waves and drought. Bergmann and others predict that environmental selection is driven from north to south by winter bottlenecks in survival, whereas Kooijman and others predict that environmental selection is driven from south to north by summer bottlenecks in production and reproduction. All the above theories ultimately are related to thermoregulation and heat exchange. While the above theories are not mutually exclusive, the integration of each may help understand and better predict endotherm response to a changing climate.

Thermoregulation is the cost of achieving heat balance. Thermoregulatory processes usually increase energy use by increasing heart rate and blood flow (e.g., vasodilation and metabolism). In hot weather, thermoregulation increases the flux of body water because water is used for evaporative cooling (e.g., panting and, to a lesser extent for *Bison*, perspiration). In cold weather, thermoregulation generates body heat (e.g., shivering, increasing metabolic heat production, and muscular activity) and conserves core body heat through control of blood flow to the periphery. Thermoregulation affects the use of energy, water, and nutrients such as electrolytes and organic nitrogen, which ultimately affects resting and foraging behaviors (Clarke 2017). High costs of energy are associated with high levels of heat transfer (e.g., thermal windows; Fig. 1) and are quantified as heat flux (W/m^2). Thermography uses long-wave infrared radiation at 7.5–14 μm to record thermal windows (FLIR Systems 2017). We used a combination of photogrammetry and thermography, known as thermogrammetry, to quantify heat flux of *Bison* during both summer and winter seasons along the Great Plains (Fig. 2) from central Saskatchewan to southeast Texas.

The Great Plains (Fig. 2) are predicted to warm (IPCC 2013, Wuebbles et al. 2017)—winters are more likely to shorten, but the longer summers are likely to be hotter with more severe droughts (Fawcett 2011, Cook et al. 2015, Cowan et al. 2017). *Bison* are resilient to short duration extreme weather events such as blizzards, dry spells, heat waves, or wildfires; however, chronic droughts and warming may affect long-term life-history traits (Martin and Barboza 2020). Moreover, anticipated warming and drying along the Great Plains will shift the distribution of vegetation types by mid- and late-century to alter the supply of digestible energy and digestible nitrogen available to *Bison*, native wildlife, and domestic livestock (Tieszen et al. 1998, Craine et al. 2015, Briske 2017).

Fig. 1. Side-by-side comparison of (left) a longwave forward looking infrared (FLIR) thermal spectrum image (pseudocolor, lighter hues are hotter (i.e., thermal windows) and darker hues are cooler) and (right) a visible wavelength spectrum photograph of the same adult male *Bison* in western Montana, summer of 2017. Emissivity = 0.94. Photo credit: Jeff M. Martin.

We use heat flux as an indicator of thermoregulatory effort to independently examine predictions from four complementary theories concerning body size and heat loads:

1. Kooijman (daily dynamic energy budget): Total body surface temperature (°C) is driven by local weather conditions,
2. Schmidt-Nielsen (surface-area-to-volume ratio): Total surface heat transfer (W) should increase over body mass (kg) and that logarithmic scaling of heat transfer and body size is allometric, predicting that $b = 0.67$,
3. Speakman and Król (heat dissipation limit affects growth): Growth rate (kg/yr) should increase with decreasing total surface heat transfer (W), and
4. Bergmann (latitudinal thermal conservatism): Heat flux (W/m^2) should increase from winter to summer and from north to south.

Finally, we test the general hypothesis that body size of endotherms is an outcome of reinforcing thermoregulatory effects on growth from immediate heat transfers to the body size eventually attained by the animal over several growing seasons in the population, that is, if all theories are supported, heat transfer processes spanning temporal and organizational scale to consistently drive body size.

Materials and Methods

Study design

We measured thermal exchange and heat loads of female *Bison* in adolescent (<3 yr) and adult (≥3 yr) age classes that were growing along the Great Plains. In addition to thermal information, we also estimated body surface area (SA; m^2) and body mass (BM_E; kg) from body height (H_E; m) using photogrammetric techniques (Martin and Barboza 2020). We observed *Bison* in 19 herds during the summer of 2017 from north to south to measure *Bison* at the hottest time of the year over 46 d from 26 June through 11 August, spending 1 d for observations at each location from Saskatchewan, Canada (52.2° N) to Texas, USA (30.7° N). We returned to 16 herds in the winter of 2017–2018 by traveling from north to south to measure *Bison* at the coldest time of the year over 38 d from 26 December through 2 February. Each of our locality visits represented the typical seasonal conditions (Appendix S1: Fig. S1). The three missed sites were excluded from follow-up observations because two were inaccessible due to blizzards (sites 1 and 2) and all the *Bison* from a third site had been removed

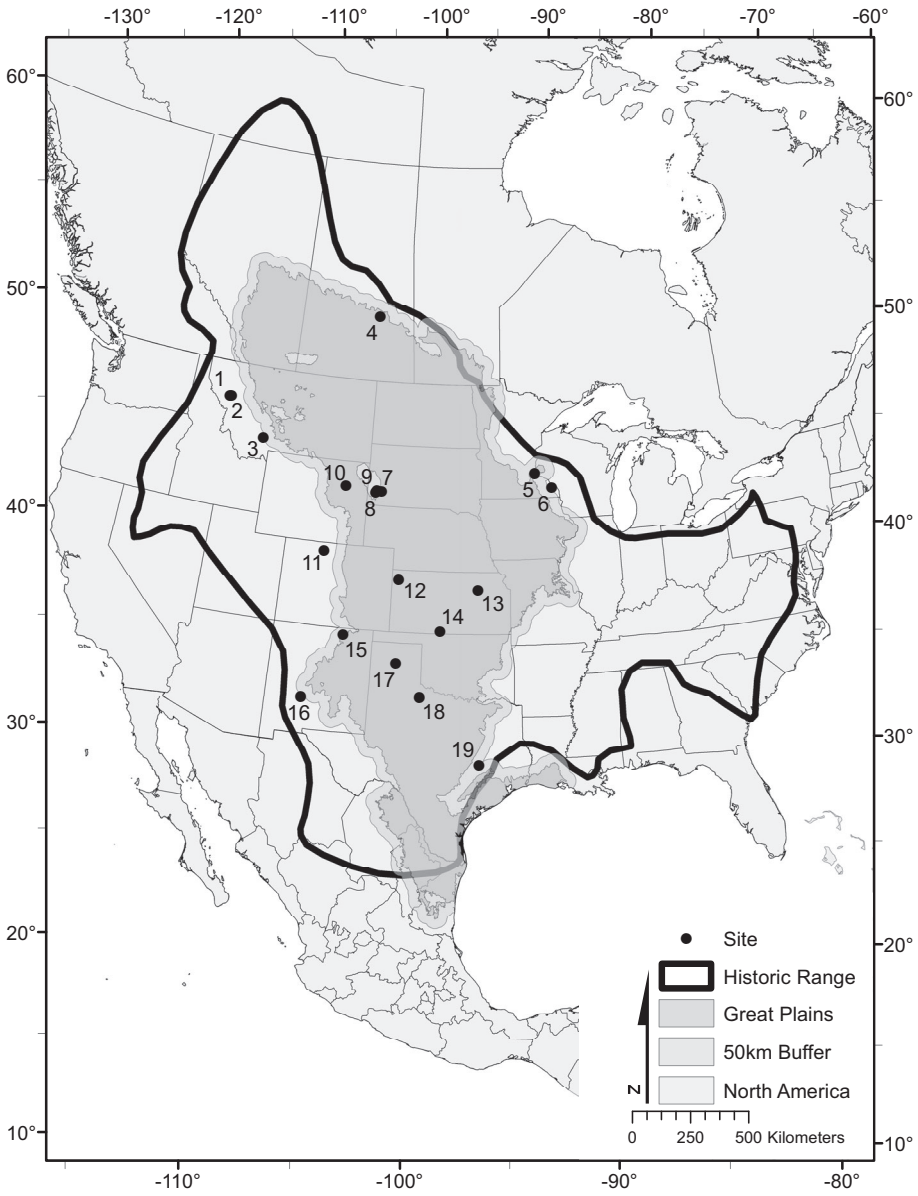

Fig. 2. Map of the Great Plains and study sites in North America. Individual site numbers correspond with Table 1. Shaded area is the Great Plains ecoregion from EPA ecoregions level I (https://www.epa.gov/eco-research/ecoregions-north-america), and the 50-km buffer is to demarcate transitional zones between other neighboring ecoregions. Historical bison range (thick solid black outline) is the pre-1870s' distribution of *Bison* traced and georeferenced from Hornaday (1889).

from the range to enclosures because natural forage had been lost to an autumn wildfire (site 9). Collectively, the sites represent a mix of management by privately owned and non-governmental organizations as well as state and federal government agencies; the sites and their respective annual climate measures are presented in Table 1.

Animal use and selection.—Studies were approved for the use of animals by the

Table 1. *Bison* site number, name, sector, state/province, mean annual temperature (MAT; °C), and mean annual precipitation (MAP; mm).

Site number	Site name	Sector	State	MAT	MAP
1†	National Bison Range, USFWS	Federal	MT	5.5	807.5
2†	Montana Buffalo Gals	Private	MT	5.5	807.5
3	Flying D	Private	MT	4.5	547.2
4	Quill Creek	Private	SK	4.8	449.9
5	Long Ago Ranch	Private	WI	7.3	942.9
6	Rockie Hill Buffalo	Private	MN	7.5	958.2
7	777 Ranch	Private	SD	8.9	482.0
8	Wind Cave National Park, NPS	Federal	SD	7.1	554.0
9‡	Custer State Park, SDGFP	State	SD	7.1	554.0
10	Durham Ranch	Private	WY	7.7	391.9
11	Eagles Wing	Private	CO	8.0	463.0
12	Beaver Creek	Private	KS	11.7	521.3
13	Konza Prairie Biological Station, TNC	NGO	KS	12.4	855.3
14	Z Bar Ranch	Private	KS	14.0	720.3
15	Vermejo Park	Private	NM	9.0	405.3
16	Armendaris Ranch	Private	NM	14.4	250.6
17	Herring Ranch	Private	TX	15.7	465.6
18	Y Ranch	Private	TX	17.8	600.2
19	Lucky B Bison	Private	TX	19.3	1230.1

Notes: Abbreviations are USFWS, United States Fish and Wildlife Service-Department of the Interior; NPS, United States National Park Service-Department of the Interior; SDGFP, South Dakota Department of Game, Fish, and Parks; and TNC, The Nature Conservancy. State abbreviations are MT, Montana; SK, Saskatchewan; WI, Wisconsin; MN, Minnesota; SD, South Dakota; WY, Wyoming; CO, Colorado; KS, Kansas; NM, New Mexico; and TX, Texas. Climate data are from NOAA (Vose et al. 2014, NOAA 2018).

† National Bison Range and adjacent private ranch, blizzard/snow storm prevented second visit in winter.

‡ Custer State Park had a fire in late 2017 (Legion Lake Wildfire), no repeat visit in winter.

Agriculture Animal Care and Use Committee (AACUC study #2017-015A; Texas A&M AgriLife Research, College Station, Texas, USA) and for the use of restricted imaging technology under Technology Control Plan (TCP #17-02-007, Texas A&M AgriLife Research). *Bison* grow over several years to achieve asymptotic body size—typically by 3 yr of age for females and by 5 yr of age for males (Martin and Barboza 2020). Environmental demands during growth of *Bison* affect asymptotic body size. Although genetic variation among bison herds exists, merely 1–2% of height variation derives from genetic variation (Musani et al. 2006, White and Wallen 2012, Licht 2017). Moreover, height and body mass are tightly related and have little variation (Martin and Barboza 2020), with 80–96% variation of body mass explained by temperature and drought; that is, large phenotypic variation is not likely due to the existing small variations in genetic makeup. Here, we focused primarily on adolescent female *Bison*, between their birth and their third year, because they shape the foundation for subsequent generations and cohorts of the population, but, when explicitly stated, adults are included as a comparison group for analyses. We categorized adolescent *Bison* into the following age classes at each site: calves ($1\ y > x$), yearlings ($1\ y \leq x < 2\ y$), and twolings ($2\ y \leq x < 3\ y$).

Thermography and photogrammetry techniques

Thermography: measure of heat exchange.—We used a forward looking infrared (FLIR) thermal imaging camera (FLIR T1030sc; FLIR Systems, Wilsonville, Oregon, USA) with a 12° × 9° lens (f/1.2) for long distance thermography. Infrared images (Fig. 1) had a fixed resolution of 1024 × 768 pixels. Camera and image calibrations were necessary for accurate and precise measures of heat exchange between each *Bison* and their environment. Seasonally, *Bison* molt their winter coats; therefore, there was a fundamental difference in the insulation factor, emissivity (ε), and reflectance (ρ) between bare skin of summer and woolly fur undercoat of winter

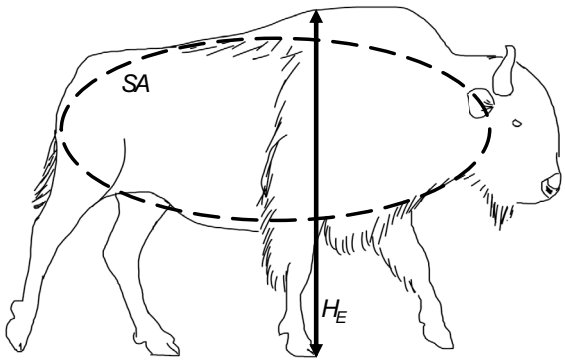

Fig. 3. Schematic of estimating size and heat flux of photographed *Bison* standing at rest in a perpendicular plane to the camera. Double black arrows indicate the estimated height (H_E; m) from the highest point on the curvature of the spine along the length of the forelimb to the ground. The ellipse indicates the effective body surface area (SA; m^2) from the ischial tuberosity to the base of the skull (posterior to the external auditory canal, clearly demarcated in thermal images) and from the dorsal plane to the ventral plane.

(see Appendix S1: Fig. S1). Emissivity values for each image were seasonally calibrated to 0.94 for *Bison* skin in summer and 0.90 for their woolly fur undercoat in winter. All measures, calculations, and model assumptions are presented in Appendix S1: Table S5. Methods for calibrating emissivity are presented in Appendix S1: Table S6. A video example is presented in Video S1.

Photogrammetry: measure of body size.—We estimated body size of *Bison* using photogrammetric methods (Berger 2012, Martin and Barboza 2020). Calculating heat flux (W/m^2) requires heat exchange over surface area (SA; m^2; Fig. 3). We calculated surface area and body height using standardized linear and area measures (Fig. 3) of *Bison* in lateral view (Martin and Barboza 2020). Optimal distance between animal and camera for most accurate height representation of the animal was determined at and around 40 m (Martin and Barboza 2020), but distance at or near 20 m was optimal for pixel coverage and density of body surfaces. We estimated body mass from body height by applying known relationships of direct measures of *Bison* body height to body mass (Martin and Barboza 2020). Similarly, calculating growth rate (kg/yr) requires a measure of body mass (BM; kg) over age (yr). To estimate rate of growth per year (kg/yr), we averaged body mass of twolings and calves for each locality, took the difference, and divided by 2 for the two-year age gap.

Thermogrammetry: measure of heat exchange and body size of Bison.—We estimated heat flux (W/m^2) between *Bison* and their environment by integrating thermographic and photogrammetric data—thermogrammetry. We extracted thermal information (e.g., temperature averages, standard deviations, minima, and maxima) of body surface area using FLIR ResearchIR Max software. Thermal data were exported for subsequent analyses to calculate net heat flux (W/m^2). We calculated total surface heat transfer (convective and radiative) using the heat calc functions as part of the Thermimage package in R (Thermimage, version 3.2.1; Tattersall et al. 2009, Tattersall 2016, 2019; R version 3.6.1, 64-bit; R Core Team 2019). However, sensible heat flux was not included in Thermimage; we thus added this term to the calculations because *Bison* are highly insulated. Sensible heat is the non-evaporative latent heat of the boundary and insulating layers related total depth of fat cover, skin thickness, and hair depth, as well as insulating characteristics of the hair (i.e., not all hair is equal for insulating; see Appendix S1: Eqs. 5 and 6). All heat flux calculations were exported as a CSV file for subsequent analyses in Stata. All parameters and assumptions for calculations in heat calc and Thermimage are presented in Appendix S1: Table S5, and the modified Thermimage code is available in the Data Access statement.

We focus on the torso of *Bison* in this study for two primary reasons: (1) It is the effective thermal window that is responsible for most of the heat transfer of the heat produced from rumination and metabolism, and (2) efficient use of time. (1) The torso is also the site where the dense cape of hair is not present, enabling the large thermal window; that is, the forequarters and head are draped in a dense coat of long guard hairs that is not shed seasonally and limits thermal exchange. However, heat transfer from appendages and horns should not be discounted (Nienaber 2009, O'Brien 2020), which leads to the next point. (2) Previous studies have captured full-body heat transfers of animals such as muskoxen (Munn et al. 2009) and sums of compartmentalized body

parts (Tattersall and Cadena 2010, Tattersall et al. 2018), but we had captured 1995 thermal images from the field, of those 779 were usable after manual digitization. Computer automation of certain BioImage informatics tasks including digitizing whole body images or body parts would increase efficiency of image processing but were not developed for this study. We acknowledge that proportional limb lengths to body height and length are important for determining heat displacement but were beyond the scope of this study.

Heat flux is a negative value when energy is emitted (i.e., heat transfer loss) from the animal to the environment. Heat transfer increases with surface temperature and solar radiant heat gain, and decreases with wind, convective, and radiative heat loss. Heat flux indicates that the animal was expending energy on thermoregulation. Heat transfer was calculated by converting mean surface temperature (T_s; °C) of *Bison* to Watts of thermal energy exchanged with their environments, including measures of ambient air temperature (dry bulb; °C), body surface reflectance (0–1), daily cloud cover (0–1), ground temperature (T_g; °C), incoming solar radiation (SE; W/m^2), wind speed (V; m/s), and convection coefficients (c, n, a, b, m) for forced and free convection flow. Conductive thermal energy is ignored because we only collected images of *Bison* in a standing posture with the soles of their hooves as the only contact with the ground. All heat flux comparison is based on black body absorbers (i.e., a perfect absorber of electromagnetic radiation), in this case a black globe temperature (T_{BG}; °C). The surface of the animal was the skin or the fur, which was always above ambient temperature and thus emitting radiant heat to the environment when compared with an inert black globe. Moving air convects heat from the animal to the environment. To estimate isometric surface-area-to-volume ratio, we fitted a regression of total surface heat transfer (W) over estimated body mass (BM_E). To test allometric scaling, we fit a log:log regression of the $\log_{10}$ of the absolute value of total surface heat transfer ($\log_{10}|W|$) and $\log_{10}$ of estimated body mass ($\log_{10}BM_E$).

Computation and statistical analyses

All thermogrammetric information, locality metadata, weather, and climate data were related and analyzed in Stata/IC (version 16.0; 64-bit; Stata, College Station, Texas, USA). We used daily measures of weather and climate as variables for converting body surface temperatures to thermal heat flux, as well as independent terms in multilevel mixed effects models. For mixed effects models, random effects were included in the models as locality to account for repeated measures of each site. Environmental variable selection for each model was parsed using the least absolute shrinkage and selection operator (or lasso) package for Stata (Tibshirani 1996). Where appropriate, model fit was assessed using either adjusted-R^2 and root square mean error of residuals (RMSE) for ordinary linear regressions or k-fold cross-validation to report the square of the correlation (pseudo-R^2) and RMSE for mixed effects models to describe model fit and strength.

Results

South of 43° N (e.g., South Dakota-Nebraska border), adolescent *Bison* between the ages of 3 months and 3 yr (n = 214) have a smaller surface area (7.8 ± 2.1 m^2), lower total surface heat transfer (−221 ± 78 W), lower body mass (271 ± 94 kg), and more heat loss (−286 ± 76 W/m^2) than their northern (n = 131) counterparts (8.9 ± 2.1 m^2; −224 ± 72 W; 324 ± 105 kg; −254 ± 67 W/m^2, respectively). Distance between animal and camera averaged 22 ± 11 m (n = 374; ranging from 8 to 68 m). Average pixel size represented 0.034 ± 0.038 m^2 (ranging from 0.003 to 0.331 m^2) of real-world size.

Body surface temperature

Body surface temperature of *Bison* averaged 38.4° ± 4.5°C in summer (n = 351) and 17.1° ± 16.6°C in winter (n = 428). Highest mean body surface temperature in summer was 48.3°C for two yearlings on a cloud-free day (0%), air temperature 34°C, relative humidity of 35%, black globe temperature 46°C, and calm wind speeds of 3.2 m/s. Lowest mean body surface temperature in winter was −55.3°C for one calf on a mostly cloudy day (63%), air temperature of −28.5°C, relative humidity of 100%, black globe temperature −14.1°C, and mild wind speed of 1.2 m/s. Body surface temperature was above or equal to average *Bison* body temperature (T_b) of

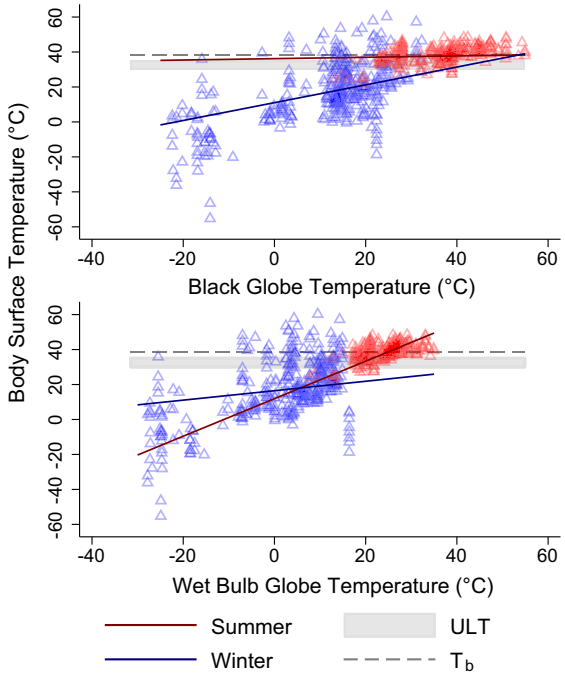

Fig. 4. Body surface temperature (°C) of *Bison* in summer (red) and winter (blue) in relation to air temperature measured as black globe temperature (°C; upper) and wet bulb globe temperature (°C; lower). Horizontal gray box indicates upper limit threshold (ULT) for black *Bos taurus* (30°C) and black *Bos indicus* (35°C). Horizontal dashed gray line represents core body temperature (T_b) for *Bison bison* (38.4°C). Cross-validation support metrics using $k_{(10)}$-fold: pseudo-R^2 = 0.61, RMSE = 10.3, N = 779 individuals, n = 19 groups by site. Random effects (site) explained 0.26% of variance.

38.4°C (Christopherson et al. 1979) in summer in 98 instances (or 67.1% of observations) and in winter in 20 instances (or 8.8% of observations). The upper limit threshold (ULT) likely ranges between 30°C and 35°C, based on ULT values for black *Bos taurus* and black *Bos indicus*, respectively (Nielsen-Kellerman 2009). Body surface temperature increased with black globe temperature (°C; i.e., solar energy) and with wet bulb globe temperature (°C; i.e., effective temperature) more quickly in winter than in summer (Fig. 4; Appendix S1: Table S1).

Components of heat exchange

Seasonal body surface temperature was related to heat flux (Fig. 5A). Heat flux comprised radiative thermal energy (difference between incoming solar gain and outgoing radiating loss; Fig. 5B), convective thermal energy (Fig. 5C), and sensible thermal energy (non-evaporative insulation; Fig. 5D). Total surface heat transfer was negatively affected by radiative heat in summer when the body surface was exposed to high radiant loads from the environment. In winter, total surface heat transfer was positively related to radiative heat; that is, radiant heat from the environment reduced total surface heat transfer from the animal (Fig. 5B). Total surface heat transfers were similarly affected by movement of air on the body surface, albeit with a greater effect in winter than in summer (Fig. 5C). The greatest range of heat fluxes (W/m^2) occurred in winter among the youngest and smallest age class. The greatest heat flux was estimated for a calf in winter at −620.8 W/m^2 when windy condition provided the highest convective loss and high cloud cover reduced radiative heat from the environment. The smallest heat flux was estimated from a calf in winter at −141.2 W/m^2 when radiative heat from the environment was low because of cloud cover and when convective losses were high due to wind.

Heat transfer

Total surface heat transfer (W) from the effective thermal window surface of the torso of *Bison* averaged −270 ± 95 W (n = 694) across both seasons; the most heat transfer was −589 W, and the least was −21 W. Total surface heat transfer (W) was linearly related to body mass of *Bison* from 44 to 745 kg (mean 335 ± 103 kg; Fig. 6, upper). The relationship between total surface heat transfer (W) and body mass (kg) was linearly related after transformation to logarithms for the allometric relationship. The slope of the log:log relationship between $\log_{10}|W|$ and $\log_{10}BM_E$ was 0.63 ± 0.03 $\log_{10}|W|\cdot\log_{10}$ kg^{-1} (95% CI: 0.57–0.69; Fig. 6, lower), which was significantly less than an isometric slope of 1.0 but consistent with the expected slope of 0.67. Results and supporting statistics for both isometric and allometric models are presented in AppendixS1: Table S2.

Total surface heat transfer varied with annual growth rates of calves and twolings (Fig. 7; Appendix S1: Table S3). Observed total surface heat transfer decreased from −340 to −207 W as

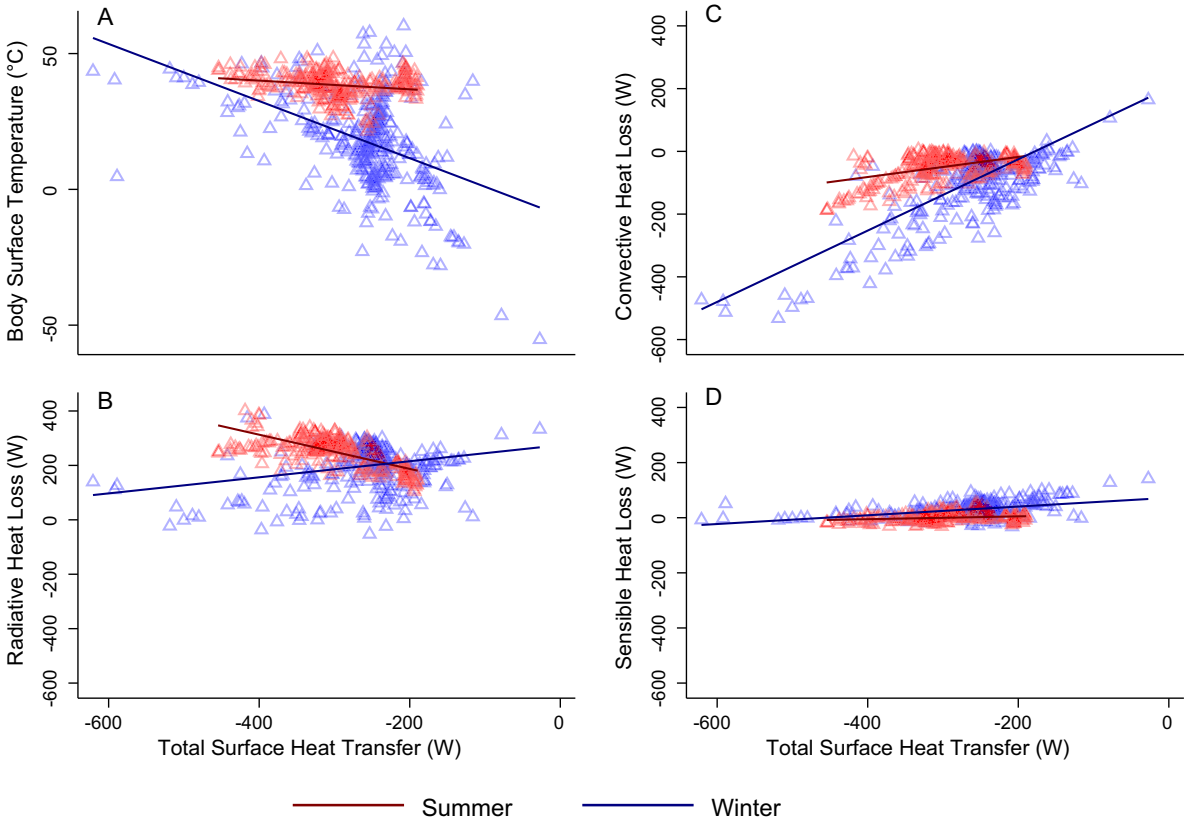

Fig. 5. Components of total surface heat transfer (W) in *Bison*. (A) Body surface temperature (°C), (B) radiative heat transfer (W; difference between incoming solar radiation and outgoing radiation), (C) convective heat transfer (W), and (D) sensible heat transfer (W).

annual growth increased from 41 to 126 kg/yr in adolescent *Bison*.

Heat flux also declined with increasing latitude in summer from −331.2 W/m^2 at 30° N in Texas to −263.5 W/m^2 at 52° N in Saskatchewan (Fig. 8). Latitudinal declines in heat flux were more pronounced in winter than in summer (Appendix S1: Table S4), that is, heat flux decreased by 3.85 ± 1.64 W/m^2 in winter and by 3.08 ± 1.66 W/m^2 in summer with each degree of latitude gained (Fig. 8).

Discussion

We used heat flux (W/m^2) and total surface heat transfer (W) as measures of thermal exchange between *Bison* and their environment along a ~2500-km transect, from Saskatchewan (52° N) to Texas (30° N) in summer and in winter. We compared four body size theories using heat flux as a common currency: Kooijman's dynamic energy budget, Schmidt-Nielsen's surface area to volume rule, Speakman and Król's heat dissipation limit, and Bergmann's rule.

Unseasonably warm winter days appear to raise surface temperatures of *Bison* (Fig. 4). The frequency of these warmer winter scenarios is expected to increase in the coming decades (Wuebbles et al. 2017), which may be stressful for large animals that are well insulated with a woolly underfur and a layer of subcutaneous fat.

Kooijman's dynamic energy budget theory predicts animals to have greater thermal loss in short-term (daily) extreme weather conditions such as high winds and extreme heat. Black globe temperature represents the effect of incoming solar radiation with ambient temperature, whereas wet blub globe temperature represents the effect of relative humidity and wind speed as ambient temperature. Our data support

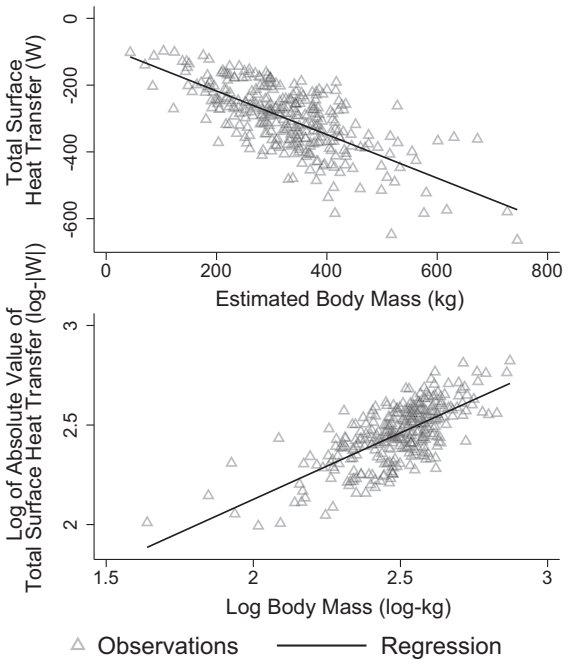

Fig. 6. Relationship between heat transfer (W) and body mass (kg) of *Bison*. Upper panel: total surface heat transfer (W) against body mass (kg) in an isometric model (ordinary least squares regression $W = ß_0 + ß\ x_1$; Adj. $R^2 = 0.31$, RMSE = 79, ß = −0.52 ± 0.03; $n = 694$ individuals). Lower panel: $\log_{10}$ absolute value of total surface heat transfer ($\log_{10}|W|$) against log body mass ($\log_{10}$kg) in an allometric model ($\log_{10}$kg; $n = 694$; $W = ß_0 \cdot x_1^{\ ß}$ $\log_{10}|W| = \log_{10} ß_0 + ß \cdot \log_{10} x_1$; ß = 0.63 ± 0.03; Adj. $R^2 = 0.36$, RMSE = 0.13, $n = 694$ individuals).

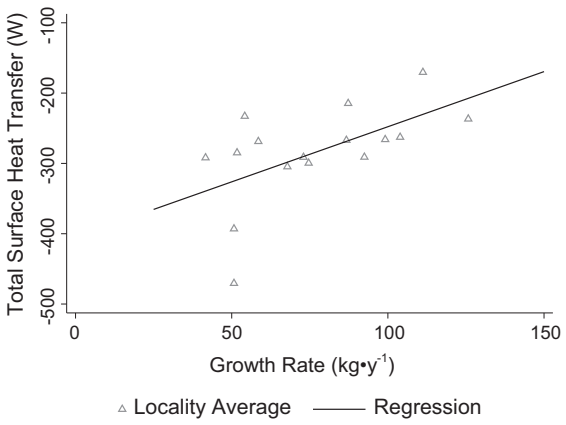

Fig. 7. Average total surface heat transfer (W) of *Bison* in relation to average growth rate (kg/yr) at each site (pseudo-$R^2 = 0.28$, RMSE = 58.6, $n = 16$ sites).

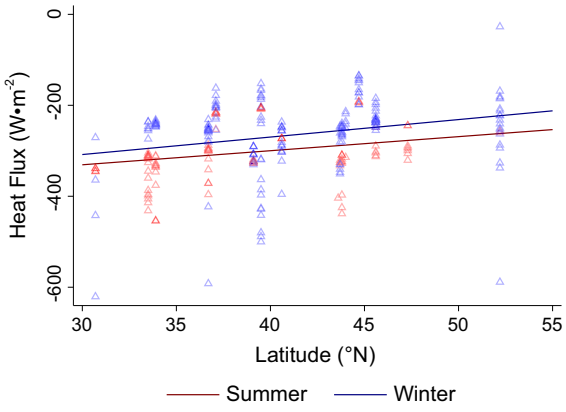

Fig. 8. Heat flux (W/m^2) of *Bison* in summer (red) and winter (blue) against latitude (°N). Cross-validation support metrics using $k_{(10)}$-fold: pseudo-$R^2 = 0.12$, RMSE = 64.6, $N = 345$ individuals, $n = 19$ groups by site. Random effects (site) explained 0.61% of variance.

Kooijman's dynamic energy budget theory (Figs. 4 and 5) because body surface temperatures were directly related to radiative loads and convective losses of energy. Schmidt-Nielsen's rule predicts that surface-area-to-volume ratio decrease with increasing body size to slow heat transfer from large animals. We found that increasing body mass increased total surface heat transfer in both an isometric and an allometric fashion (Fig. 6). The isometric model predicted greater heat transfer than was observed for the smallest 5% of *Bison* (≤164 kg; −162 W vs. −138 W), whereas estimates from the allometric model were not significantly different; this was tested by using a paired t-test of the observed and predicted heat transfer values of the smallest and the largest 5% (≥511 kg) of *Bison*. Speakman and Król's heat dissipation limit theory predicts that production is suppressed when heat loads from the environment and metabolism divert energy to thermoregulation. Our data demonstrate that growth of *Bison* is limited by heat loads because the slowest annual growth rates were associated with the greatest heat transfer (Fig. 7). However, we acknowledge that the temporal resolution of growth data is too large to resolve the relationship of growth and excessive heat loads within a growing season. Bergmann's rule predicts that selection favors large animals at higher latitudes. The ability to retain heat in

cold winters (sensu Schmidt Nielsen; Fig. 6) has been invoked as an explanation for Bergmann's rule. Our data provide some support for thermal conservatism, because heat flux from the smallest 5% of *Bison* (≤164 kg; $-248 + 58$ W/m^2) was greater than that of the largest 5% of *Bison* (≥511 kg; -230 ± 30 W/m^2). However, Bergmann's rule is also explained by summer growth and the net primary production of food (Huston and Wolverton 2011). Asymptotic size of *Bison* on the Great Plains declines with high decadal temperatures and droughts that suppress growth of both the animal and the forages they consume (Martin and Barboza 2020). In this study, high annual growth rates were observed at high and low latitudes at sites with mean annual precipitation above 450 mm (Table 1; Fig. 7), which suggests that growth is dependent on thermal exchanges as well as forage supplies.

Our study of heat transfers in bison provided support for all four theories of body size, which suggests that body size is an outcome of consistent effects across temporal and organizational scales from instantaneous heat balance through seasonal growth of this long-lived animal. Reinforcement between levels of organization multiplies the effect of body size of individuals in a population on other ecological processes especially for large keystone species such as bison that influence the composition of plant and animal communities in their ecosystem (White 1983, Knapp et al. 1999, Beschta et al. 2020).

Conservation implications

Annual and seasonal mean temperatures are expected to rise over the next eight decades, and this will increase heat loads and thus increase negative heat transfer. Increasing negative heat transfer will further decrease growth rates and likely alter life-history traits (Martin and Barboza 2020) including reproduction rates. Special conservation and management considerations by organizations like the IUCN-SSC Bison Specialist Group, conservation NGOs like The Nature Conservancy, state and federal bison herd managers like the National Park Service, and private bison herd managers will need to be given to the central and southern Great Plains where the number of extremely hot days (>32°C) is expected to rise to 87 d/yr from 32 d/yr (Weatherly and Rosenbaum 2017). Marginal habitats will also challenge conservation plans in places like the arid desert regions of the American southwest where drought is expected to be persistent, lengthening, and intensifying and expanding into new areas like the central Great Plains (Cook et al. 2015).

Conclusions

Cooler summers are more optimal for *Bison* growth because of reduced heat loads during the growing season. Rising temperatures constrain body size and productivity of *Bison*. We report five key findings:

1. Daily measures of weather—wind speed, heat index, solar radiation, relative humidity—affect heat flux of endotherms seasonally; our study supports Kooijman's dynamic energy budget hypothesis (Fig. 4).
2. Heat transfer is allometric with body size ($b = 0.63$) and thus consistent with Schmidt-Nielsen prediction of $b = 0.67$ (or the two-thirds rule) that mass-specific heat transfer declines with increasing body size (Fig. 6).
3. Annual growth declined with increasing heat flux, which supports Speakman and Król's heat dissipation limit hypothesis (Fig. 7).
4. Winter and summer seasons appear to conform to Bergmann's rule, where *Bison* conserve heat in cooler-northern locations (Fig. 8).
5. The confirmation of the above four theories, using heat flux as a common currency, suggests that an integrated general theory of thermoregulation could be developed with additional studies of other taxa following the framework put forth in this study.

Acknowledgments

Managers and owners of the 19 study herds were generous in providing exceptional hospitality and engaging discussions with JMM during his fieldwork, especially Tom and Kris Martin. We especially thank Rachel Short for her enduring support during JMM's travels and her excellent map making skills for Fig. 2. We also recognize Jim I. Mead and the Mammoth Site of Hot Springs, SD for providing extended housing and logistics during JMM's fieldwork. Mike Jacobson of North American Bison, LLC in New Rockford, North Dakota, was especially helpful, providing data and information on slaughtered bison body components. JMM is specifically thankful for the in-kind donations of

bison-hair-insulated gear provided in part by United by Blue, The Buffalo Wool Co., and Buffalo Gold/Herd Wear, especially for the exceptionally cold winter weather of the northern Great Plains. Stipends for JMM were provided by the Boone & Crockett Club | Dr. James "Red" Duke Endowment for Wildlife Conservation and Policy at Texas A&M University. Research and travel funding was provided in part by the Western Bison Association research grant, the 2018 Rolex Explorer Grant at the Explorers Club, the Throlson American Bison Foundation Scholarship at the National Bison Association, and the Larry D. Agenbroad Legacy Fund at The Mammoth Site, the Boone & Crockett Club | Dr. James "Red" Duke Wildlife Science to Policy Program at Texas A&M University, the Graduate Student Association of Wildlife and Fisheries Sciences Department at Texas A&M University, the Office of Graduate and Professional Students at Texas A&M University, and the Graduate and Professional Student Government at Texas A&M University. The authors declare that they have no conflict of interest. JMM conceived the ideas and designed methodology. JMM collected the data. JMM and PSB interpreted and analyzed the data. JMM and PSB drafted, revised, and approved the final manuscript. Both authors contributed critically to the drafts and gave final approval for publication.

Literature Cited

Berger, J. 2012. Estimation of body-size traits by photogrammetry in large mammals to inform conservation. Conservation Biology 26:769–777.

Bergmann, C. 1847. Über die verhältnisse der warmeokonomie der thiere zu ihrer größe (translation: on the conditions of the thermal economy of animals to their size). Göttinger Studien, Göttingen, Germany.

Beschta, R. L., W. J. Ripple, J. B. Kauffman, and L. E. Painter. 2020. Bison limit ecosystem recovery in northern Yellowstone. Food Webs 23:e00142.

Briske, D. D., editor. 2017. Rangeland systems: processes, management and challenges. Springer Nature, Cham, Switzerland.

Christopherson, R. J., R. J. Hudson, and M. K. Christophersen. 1979. Seasonal energy expenditures and thermoregulatory responses of bison and cattle. Canadian Journal of Animal Science 59:611–617.

Clarke, A. 2017. Principles of thermal ecology: temperature, energy and life. Oxford University Press, New York, New York, USA.

Clauss, M., M. T. Dittmann, D. W. H. Müller, C. Meloro, and D. Codron. 2013. Bergmann's rule in mammals: a cross-species interspecific pattern. Oikos 122:1465–1472.

Cook, B. I., T. R. Ault, and J. E. Smerdon. 2015. Unprecedented 21st century drought risk in the American Southwest and Central Plains. Science Advances 1:e1400082.

Cowan, T., G. C. Hegerl, I. Colfescu, M. Bollasina, A. Purich, and G. Boschat. 2017. Factors contributing to record-breaking heat waves over the great plains during the 1930s Dust Bowl. Journal of Climate 30:2437–2461.

Craine, J. M., E. G. Towne, M. Miller, and N. Fierer. 2015. Climatic warming and the future of bison as grazers. Scientific Reports 5:16738.

Fawcett, P. J., et al. 2011. Extended megadroughts in the southwestern United States during Pleistocene interglacials. Nature 470:518–521.

FLIR System. 2017. Use low-cost materials to increase target emissivity. https://www.flir.com/discover/rd-science/use-low-cost-materials-to-increase-target-emissivity/

Hornaday, W. T. 1889. The extermination of the American Bison. Government Printing Office, Washington, D.C., USA.

Huston, M. A., and S. Wolverton. 2011. Regulation of animal size by eNPP, Bergmann's rule, and related phenomena. Ecological Monographs 81:349–405.

IPCC. 2013. Climate change 2013: the physical science basis. *In* T. F. Stocker, D. Qin, G.-K. Plattner, M. Tignor, S. K. Allen, J. Boschung, A. Nauels, Y. Xia, V. Bex and P. M. Midgley, editors. Contribution of Working Group I to the Fifth Assessment Report of the Intergovernmental Panel on Climate Change. Cambridge University Press, Cambridge, UK and New York, New York, USA, 1535 pp.

Kearney, M. 2012. Metabolic theory, life history and the distribution of a terrestrial ectotherm. Functional Ecology 26:167–179.

Knapp, A. K., J. M. Blair, J. M. Briggs, S. L. Collins, D. C. Hartnett, L. C. Johnson, E. G. Towne, M. John, and L. Scott. 1999. The keystone role of *Bison* in North American tallgrass prairie. BioScience 49:39–50.

Kooijman, S. A. L. M. 2000. Dynamic energy and mass budgets in biological systems. Second edition. Cambridge University Press, Cambridge, UK.

Licht, D. S. 2017. Bison conservation in Northern Great Plains National Parks: no need to panic. Great Plains Research 27:83–92.

Martin, J. M., and P. S. Barboza. 2020. Decadal heat and drought drive body size of North American bison (*Bison bison*) along the Great Plains. Ecology and Evolution 10:336–349.

Martin, J. M., J. I. Mead, and P. S. Barboza. 2018. Bison body size and climate change. Ecology and Evolution 8:4564–4574.

Munn, A. J., P. S. Barboza, and J. Dehn. 2009. Sensible heat loss from Muskoxen (*Ovibos moschatus*) feeding in winter: Small calves are not at a thermal disadvantage compared with adult cows. Physiological and Biochemical Zoology 82:455–467.

Musani, S. K., N. D. Halbert, D. T. Redden, D. B. Allison, and J. N. Derr. 2006. Marker genotypes and population admixture and their association with body weight, height and relative body mass in United States federal bison herds. Genetics 174:775–783.

Nielsen-Kellerman. 2009. Kestrel: 5400AG cattle heat stress tracker. Nielsen-Kellerman, Boothwyn, Pennsylvania, USA.

Nienaber, J. 2009. Validation and application of infrared thermography for the assessment of body condition in Pinnipeds. University of Alaska Fairbanks, Fairbanks, Alaska, USA.

NOAA. 2018. Climate at a Glance. https://www.ncdc.noaa.gov/cag/divisional/time-series.

O'Brien, H. D. 2020. From anomalous arteries to selective brain cooling: parallel evolution of the artiodactyl carotid rete. Anatomical Record 303:308–317.

R Core Team. 2019. R: a language and environment for statistical computing. R foundation for statistical computing, Vienna, Austria.

Schmidt-Nielsen, K. 1970. Energy metabolism, body size, and problems of scaling. Federation Proceedings 29:1524–1532.

Speakman, J. R., and E. Król. 2010. Maximal heat dissipation capacity and hyperthermia risk: neglected key factors in the ecology of endotherms. Journal of Animal Ecology 79:726–746.

Speakman, J. R., and E. Król. 2011. Limits to sustained energy intake. XIII. Recent progress and future perspectives. Journal of Experimental Biology 214:230–241.

Tattersall, G. J. 2016. Infrared thermography: a non-invasive window into thermal physiology. Comparative Biochemistry and Physiology - A Molecular and Integrative Physiology 202:78–98.

Tattersall, G. J. 2019. Thermimage: thermal image analysis. CRAN. http://doi.org/10.5281/zenodo.1069704

Tattersall, G. J., D. V. Andrade, and A. S. Abe. 2009. Heat exchange from the toucan bill reveals a controllable vascular thermal radiator. Science 325:468–470.

Tattersall, G. J., and V. Cadena. 2010. Insights into animal temperature adaptations revealed through thermal imaging. Imaging Science Journal 58:261–268.

Tattersall, G. J., J. A. Chaves, and R. M. Danner. 2018. Thermoregulatory windows in Darwin's finches. Functional Ecology 32:358–368.

Tibshirani, R. 1996. Regression shrinkage and selection via the lasso. Journal of the Royal Statistical Society 58:267–288.

Tieszen, L. L., L. Stretch, and J. Vander Kooi. 1998. Stable isotopic determination of seasonal dietary patterns in bison at four preserves across the Great Plains. Pages 130–140 *in* L. R. Irby and J. E. Knight, editors. Proceedings of the International Symposium on Bison Ecology and Management in North America. Extension Wildlife Program, Montana State University, Bozeman, Montana, USA.

Vose, R. S., S. Applequist, M. Squires, I. Durre, M. J. Menne, J. Williams, N. Claude, C. Fenimore, K. Gleason, and D. Arndt. 2014. NOAA's Gridded Climate Divisional dataset (CLIMDIV). https://doi.org/10.7289/V5M32STR

Weatherly, J. W., and M. A. Rosenbaum. 2017. Future projections of heat and fire-risk indices for the contiguous United States. Journal of Applied Meteorology and Climatology 56:863–876.

White, P. J., and R. L. Wallen. 2012. Yellowstone bison-should we preserve artificial population substructure or rely on ecological processes? Journal of Heredity 103:751–753.

White, R. G. 1983. Foraging patterns and their multiplier effects on productivity of northern ungulates. Oikos 40:377–384.

Wuebbles, D. J., D. W. Fahey, K. A. Hibbard, D. J. Dokken, B. C. Stewart, and T. K. Maycock. 2017. Climate science special report: fourth National Climate Assessment. U.S. Global Change. Research Program 1:470.

Data Availability Statement

Data are available on Figshare data repository (Martin and Barboza 2020). https://doi.org/10.6084/m9.figshare.12084645.

Supporting Information

Additional Supporting Information may be found online at: http://onlinelibrary.wiley.com/doi/10.1002/ecs2.3176/full